Structurally Characterized Mesostructured Hybrid Surfactant−Inorganic Lamellar Phases Containing the Adamantane $[Ge_4S_{10}]^{4-}$ Anion: Synthesis and Properties

François Bonhomme and Mercouri G. Kanatzidis*

Department of Chemistry and Center for Fundamental Materials Research, Michigan State University, East Lansing, Michigan 48824

Received November 17, 1997. Revised Manuscript Received January 30, 1998

The reaction of aqueous solutions of $Na_4Ge_4S_{10}$ with various surfactant alkyltrimethylammonium bromide salts yielded new surfactant−inorganic phases containing the adamantane thiogermanate anion $[Ge_4S_{10}]^{4-}$. The resulting $[C_nH_{2n+1}N(CH_3)_3]_4Ge_4S_{10}$ phases with $n = 12$, 14, 16, and 18 crystallize in the triclinic space group *P*-1 and contain parallel inorganic planes of unconnected $[Ge_4S_{10}]^{4-}$ clusters, separated at mesoscopic scale lengths by organic bilayers of interdigitated cationic surfactant chains. These air-stable compounds were characterized by thermal analyses, Raman, far-IR, and solid-state UV−vis reflectance spectroscopy. Their ability to absorb reversibly various alcohols was studied by in-situ X-ray powder diffraction.

Introduction

Compounds composed of segregated layers of inorganic anions and organic cations are now of considerable interest[1] because of the recognition that the arrangement and spacings of the anions can be controlled by the size and shape of the cations and vice versa.[2] The ability to vary the spacing, and thus the coupling, between anion planes can lead to phases with interesting shape-selective, structural, electrical, and magnetic properties, found, for example, among the alkylammonium tetrahalogenometalates studied in the sixties and seventies.[3,4] These phases often exhibit complicated phase diagrams with order/disorder solid-state phase transitions occurring at relatively low temperature.[5−7] Another exemplary class of compounds is the so-called charge-transfer salts, which contain small inorganic anions sandwiched between layers of, for example, partially oxidized organo-chalcogen donor molecules.[8] These "organic−inorganic molecular composites"[9] can be semiconductors, metals, or even superconductors. The synthesis of a new class of molecular sieves[10] by a liquid-crystal template approach and the increasing interest in soft chemical methods paved the way to the discovery of various new surfactant templated transition metal oxides.[11−14] Very recently,[15] vanadium oxide dodecylamine was obtained hydrothermally, and for the first time, the structure of such an oxide was elucidated. In fact, very few structures containing inorganic ions and long surfactant chains have been accurately determined to date. They mostly concern the tetrahalometalates of general formula $[C_nH_{2n+1}NH_3]_2MX_4$ (M = Mn, Cu, Co, etc., X = Cl, Br).[16−18] Similarly, among the alkyltrimethylammonium surfactants, only $C_{16}H_{33}N(CH_3)_3Br$ was structurally characterized.[19]

Microporous sulfides with framework topologies resembling those of zeolites have been forecast by Bedard et al.,[20] and several such compounds were discovered in the recent years.[21−24] By analogy with the silicates, where the elemental structural building units are $[SiO_4]^{4-}$ tetrahedra, these sulfides usually contain the adamantane thioanion $[Ge_4S_{10}]^{4-}$ built up by four

(1) (a) Ouahab, L. *Chem. Mater.* **1997**, *9*, 1909. (b) Clemente-León, M.; Mingotaud, C.; Agricole, C.; Gómez-García, J.; Coronado, E.; Delhaès, P. *Angew. Chem., Int. Ed. Engl.* **1997**, *36*, 1114.
(2) (a) Lehn, J. M. *Supramolecular Chemistry*; VCH: Weinheim, 1995. (b) Kanatzidis, M. G. *Phosphorous, Sulfur Silicon* **1994**, *93*−*94*, 159.
(3) Koppen, J.; Hamersma, R.; Lebesque, J. V.; Miedema, A. R. *Phys. Lett.* **1967**, *25A*, 376.
(4) Peterson, E. R.; Willet, R. D. *J. Chem. Phys.* **1972**, *56*, 1879.
(5) Landi, E.; Vacatello, M. *Thermochimica Acta* **1975**, *12*, 141.
(6) Landi, E.; Vacatello, M. *Thermochimica Acta* **1975**, *13*, 441.
(7) Carla, A.; Giuseppe, M.; Giuseppe, Z. *J. Phys. Chem.* **1986**, *90*, 852.
(8) Day, P.; Kurmoo, M. *J. Mater. Chem.* **1997**, *7* (8), 1291.
(9) Day, P. *Philos. Trans. R. Soc. London A* **1985**, *314*, 145.
(10) Kresge, C. T.; Leonowicz, M. E.; Roth, W. J.; Vartuli, J. C.; Beck, J. S. *Nature* **1992**, *359*, 710.
(11) Huo, Q.; Margolese, D. I.; Clesla, U.; Feng, P.; Gier, T. E.; Sieger, P.; Leon, R.; Petroff, P. M.; Schuth, F.; Stucky, G. D. *Nature* **1994**, *28*, 317.
(12) Janauer, G. G.; Dobley, A.; Guo, J.; Zavalij, P.; Whittingham, M. S. *Chem. Mater.* **1996**, *8*, 2096.
(13) Stein, A.; Fendorf, M.; Jarvie, T. P.; Mueleer, K. T.; Benesi, A. J.; Mallouk, T. E. *Chem. Mater.* **1995**, *7*, 304.
(14) Huo, Q.; Margolese, D. I.; Ciesla, U.; Demuth, D. G.; Feng, P.; Gier, T. E.; Sieger, P.; Firouzi, A.; Chmelka, B. F.; Schuth, F.; Stucky, G. D. *Chem. Mater.* **1994**, *6*, 1176.
(15) Janauer, G. G.; Dobley, A.; Zavalij, P.; Whittingham, M. S. *Chem. Mater.* **1997**, *9*, 647.
(16) Ciajolo, M. R.; Corradini, P.; Pavone, V. *Gazz. Chim. Ital.* **1976**, *106*, 807.
(17) Ciajolo, M. R.; Corradini, P.; Pavone, V. *Acta Crystallogr.* **1977**, *B33*, 553.
(18) Guo, N.; Lin, Y.-H.; Xi, S.-Q. *Acta Crystallogr.* **1995**, *C51*, 617.
(19) Campanelli, A. R.; Scaramuzza, L. *Acta Crystallogr.* **1986**, *C42*, 1380.
(20) Bedard, R. L.; Wilson, S. T.; Vail, L. D.; Bennett, J. M.; Flanigen, E. M. *Zeolites, Facts, Figures, Future. Proceedings of the 8th International Zeolite Conference*; Elsevier: Amsterdam, 1989; p 375.
(21) Yaghi, O. M.; Sun, Z.; Richardson, D. A.; Groy, T. L. *J. Am. Chem. Soc.* **1994**, *116*, 807.
(22) Parise, J. B.; Tan, K. *Chem. Commun.* **1996**, *14*, 1687.
(23) Cahill, C. L.; Parise, J. B. *Chem. Mater.* **1997**, *9*, 807.
(24) Bowes, C. L.; Ozin, G. A. *Adv. Mater.* **1996**, *8*, 13.

S0897-4756(97)00755-2 CCC: $15.00
Published on Web 03/13/1998

corner-linked $[GeS_4]^{4-}$ tetrahedra. These adamantane clusters are quite stable in water and are therefore well suited for ion-exchange type reactions with soluble cationic templates. Because they can serve as precursors for the construction of micro- and mesoporous sulfidic phases, we have studied in detail their corresponding salts with surfactants. An assessment of the ability of these lone cations to arrange and organize in space, using accurately determined structures of the surfactant precursors, will help our understanding of the formation of mesoporous phases and should help us utilize these surfactant templates more efficiently. Furthermore, structural information on surfactant-based phases could be used to construct more accurate models for representing self-assembled monolayers and lipid bilayers.

We have prepared and crystallized new phases of $[Ge_4S_{10}]^{4-}$ with several surfactant alkyltrimethylammonium cations, and we report in this paper the synthesis, structure, and spectroscopic and physicochemical properties of the hybrid thiogermanates−surfactant phases $[C_nH_{2n+1}N(CH_3)_3]_4Ge_4S_{10}$ with $n = 12$, 14, 16, and 18, (hereafter designated C*n*GS).

Experimental Section

Reagents. Chemicals were used as obtained: (i) germanium powder 99.999% purity, −100 mesh, Alfa Aesar; (ii) sulfur powder, sublimed, J. T. Baker Chemical Co.; (iii) sodium metal, 98%, Spectrum Chemical; (iv) dodecyltrimethylammonium bromide (C12Br), 99%, TCI America; (v) tetradecyltrimethylammonium bromide (C14Br), 99%, Aldrich Chemical; (vi) hexadecyltrimethylammonium bromide (C16Br), 98%, Alfa Avocado; (vii) octadecyltrimethylammonium bromide (C18Br), Fluka Chemika; (viii) ethanol, ACS anhydrous, EM Science, Inc.; (ix) diethyl ether, ACS anhydrous, EM Science, Inc.; (x) acetone, ACS anhydrous, EM Science, Inc.

Synthesis. Na_2S was prepared by reacting stoichiometric amounts of the elements in liquid ammonia as described elsewhere.[25] $Na_4Ge_4S_{10}$[26] was prepared by heating in evacuated quartz tubes stoichiometric amounts of thoroughly mixed Na_2S, Ge, and S at 850 °C for 48 h. This procedure gave a very hygroscopic, pale-yellow crystalline translucent phase, which was stored in a nitrogen-filled glovebox.

The C*n*GS phases were prepared in aqueous solutions at room temperature according to the following ion-exchange reaction:

$$4C_nH_{2n+1}N(CH_3)_3Br + Na_4Ge_4S_{10} \rightarrow [C_nH_{2n+1}N(CH_3)_3]_4Ge_4S_{10} + 4NaBr$$

The C*n*Br surfactants were dissolved by stirring in distilled water, at room temperature for C12Br and C14Br and at about 40 °C for C16Br and C18Br. The resulting surfactant concentration was typically 5 wt %.

$Na_4Ge_4S_{10}$ dissolves readily in water at room temperature. A small amount of insoluble impurities (unreacted sulfur and germanium) was filtered off. This transparent yellowish solution was then added upon vigorous stirring to the clear surfactant solution, giving off immediately an abundant white precipitate. This slurry was stirred for 1 h and then allowed to stand overnight. The precipitate was then filtered, was washed copiously with water, then with ethanol, and finally with ether, and was vacuum-dried at room temperature overnight. The resulting whitish powder has a soapy texture, is stable in air for many months, and is not hygroscopic. A typical yield based on $Na_4Ge_4S_{10}$ is 85%. Different starting concentrations of surfactants in water were tried, ranging from 2 wt % to 30 wt %, but gave the same final product.

Physical Measurements. *Powder X-ray Diffraction.* Analyses were performed using a computer-controlled INEL CPS120 powder diffractometer in asymmetric reflection mode, operating at 40 kV/20 mA, with a graphite-monochromatized Cu Kα radiation. The diffractometer was calibrated in the low-angle region using hexadecyltrimethylammonium bromide (C16Br)[19] as external standard.

Infrared Spectroscopy. Infrared spectra, in the far-IR region (600−100 cm^{-1}), were recorded on a computer-controlled Nicolet 750 Magna-IR Series II spectrometer equipped with a TGS/PE detector and a silicon beam splitter in 4 cm^{-1} resolution. The samples were mixed with ground dry KBr and pressed into translucent pellets.

Raman Spectroscopy. Raman spectra, in the far-Raman region (1000−100 cm^{-1}) were recorded with a BIO-RAD FT Raman spectrometer with a Spectra-Physics Topaz T10-106c 1.064 nm YAG laser. The pure samples were loaded without preparation into melting point capillary tubes.

Solid-State UV/Vis/Near-IR Spectroscopy. Optical diffuse reflectance measurements were performed at room temperature using a Shimadzu UV-3101PC double beam, double monochromator spectrophotometer equipped with an integrating sphere. $BaSO_4$ was used as a 100% reflectance standard for all measurements. Samples are prepared by spreading them on a compacted surface of the powdered standard material, preloaded into a sample holder. The reflectance versus wavelength data generated can be used to estimate the band gap of a material by converting reflectance to absorption data as described earlier.[25]

Thermogravimetric Analyses (TGA). TGA data were obtained with a computer-controlled Shimadzu TGA-50 thermal analyzer. Typically 40 mg of sample was placed in a quartz bucket and heated in a nitrogen flow of 50 mL/min at 2 °C/min. The end products of the TGA experiments were examined by X-ray powder diffraction.

Differential Scanning Calorimetry (DSC). DSC experiments were performed on a computer-controlled Shimadzu DSC-50 thermal analyzer. About 10 mg of sample was sealed under nitrogen in an aluminum container. A similar container filled with an equal amount of Al_2O_3 is used as reference. All the measurements were done with a heating rate of 2 °C/min.

Semiquantitative Microprobe Analyses (EDAX). The analyses were performed using a JEOL JSM-6400V scanning electron microscope equipped with a TN 5500 EDS detector. Data acquisition was performed with an accelerating voltage of 20 kV and 20 s accumulation time.

Single-Crystal X-ray Crystallography. Intensity data for all four phases were collected on a Siemens SMART-CCD diffractometer using graphite-monochromatized Mo Kα radiation. Each data collection covered over a hemisphere of reciprocal space, up to about 46° in 2θ. The individual frames were measured with an ω rotation of 0.3° and an acquisition time of 10 s, leading to a total measurement time of about 6 h per data set. The SMART software[27] was used for the data acquisition, SAINT[27] for data extraction and reduction, SADABS[27] for absorption correction, and SHELXTL[28] for structure solution and refinement. The calculations were performed on a Silicon Graphics Iris Indigo workstation.

Results and Discussion

Synthesis and Crystallization. The powder diffraction patterns of these compounds, given in Figure 1, are reminiscent of those of "lamellar phases", showing

(25) McCarthy, T. J.; Ngeyi, S.-P.; Liao, J.-H.; DeGroot, D. C.; Hogan, T.; Kannewurf, C. R.; Kanatzidis, M. G. *Chem. Mater.* **1993**, *5*, 331.

(26) Philippot, E.; Ribes, M.; Lundqvist, O. *Revue de Chimie Minérale* **1971**, *8*, 477.

(27) *SMART and SAINT* (Data collection and Processing Software for the SMART-CCD system); Siemens Analytical X-ray Instruments Inc.: 1995.

(28) *SHELXTL Version 5, Reference Manual*; Siemens Industrial Automation Inc.: 1994.

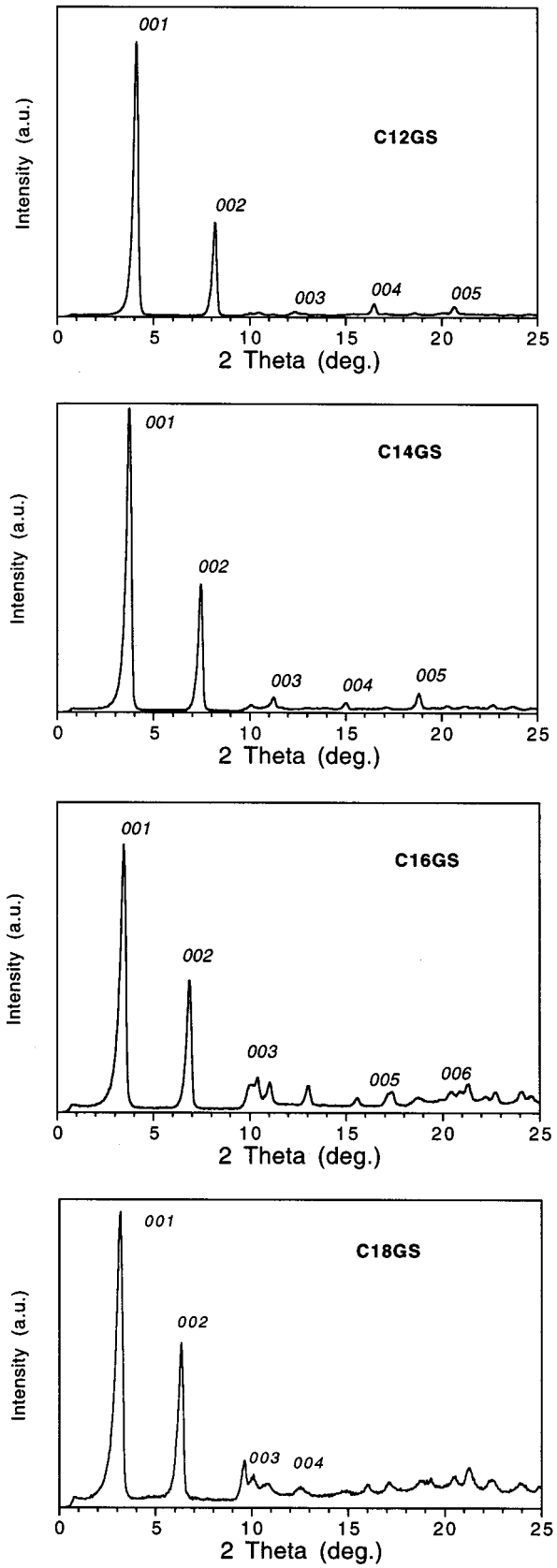

Figure 1. X-ray powder diffraction patterns of C12GS, C14GS, C16GS, and C18GS.

mostly 00*l* type reflections and are affected by preferred orientation. The interlayer spacings of the C*n*GS phases are only slightly bigger than the ones of the corresponding surfactants C*n*Br and increase similarly with *n*, as shown in Figure 2. Semiquantitative EDAX

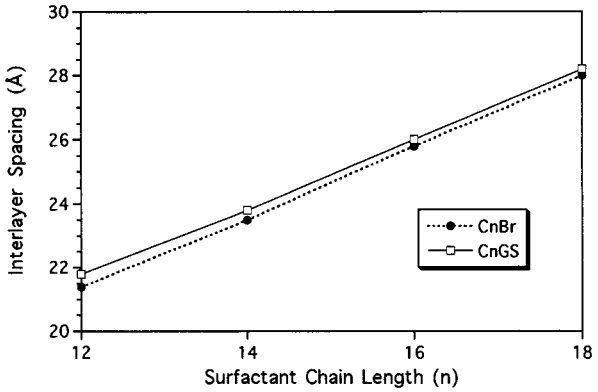

Figure 2. Variation of the interlayer spacing of C*n*GS and C*n*Br with *n*.

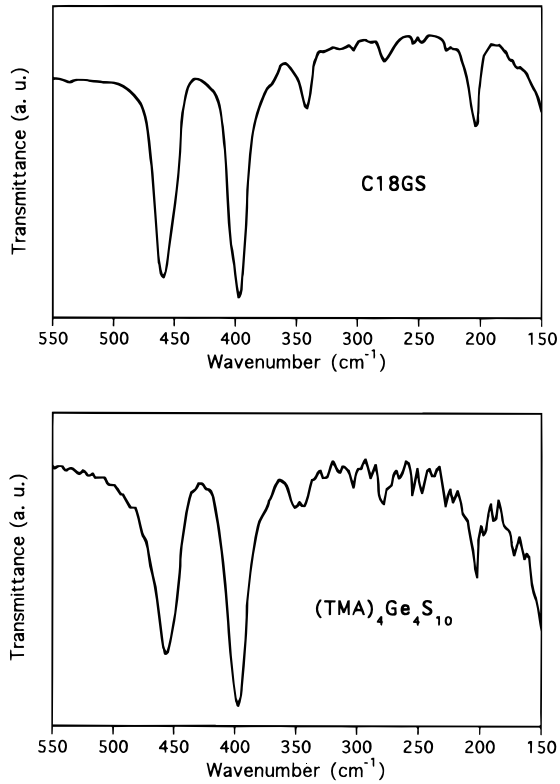

Figure 3. Far-IR spectra of C18GS and $[(CH_3)_4N]_4Ge_4S_{10}$.

showed that no remaining Br or Na was present in the samples and that their S to Ge atomic ratio was close to 2.5. Their far-IR or Raman spectra were identical to each other and similar to those of $Na_4Ge_4S_{10}$ or $((CH_3)_4N)_4Ge_4S_{10}$ [29] (see Figures 3 and 4, respectively), showing that the adamantane $[Ge_4S_{10}]^{4-}$ cluster was indeed present and still intact. The solid-state UV−vis diffuse reflectance spectra of the C*n*GS phases taken at room temperature, shown in Figure 5 for C16GS, exhibit a sharp decline in reflectance around 350 nm, indicating that these compounds are insulators, with a band gap of approximately 3.6 eV. The corresponding optical spectrum of $((CH_3)_4N)_4Ge_4S_{10}$ is very similar with a gap of ∼3.55 eV.

The synthetic method used led to pure phases, but only in microcrystalline form, clearly unsuitable for

(29) Pivan, J. Y.; Achak, O.; Louër, M.; Louër, D. *Chem. Mater.* **1994**, *6*, 827.

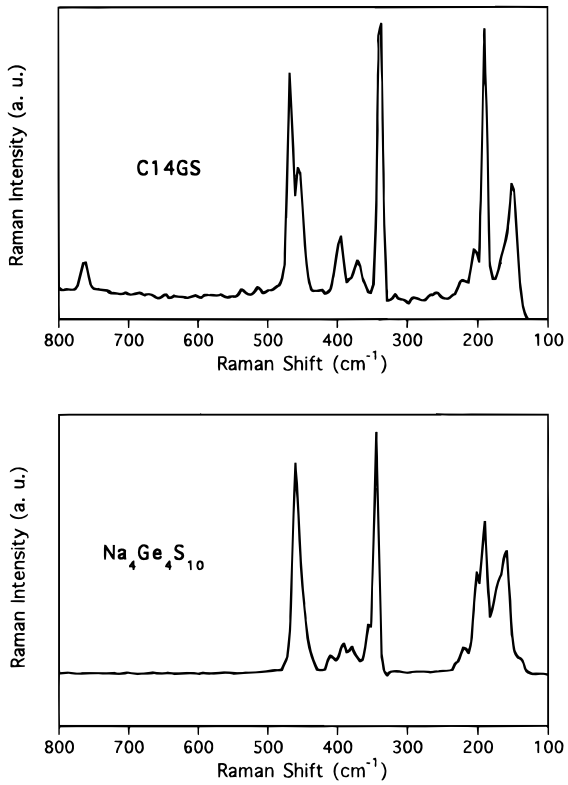

Figure 4. Raman spectra of C14GS and $Na_4Ge_4S_{10}$.

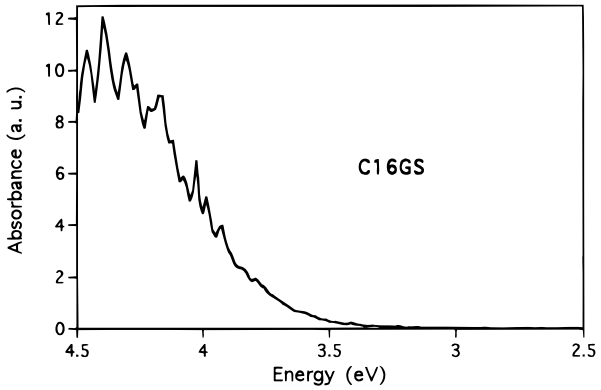

Figure 5. Solid-state UV−vis reflectance spectrum of C16GS.

structural analyses. Starting with the dry precipitate, very good single crystals were obtained by two different methods. The C*n*GS phases are slightly soluble around room temperature in ethanol/water or acetone/water mixtures. Typically 100 mg of compound was dissolved by sonication in 50 mL of a 5:1 (by volume) ethanol/water solution at about 35 °C. Upon cooling in an open beaker, transparent colorless single crystals of C14GS with plate morphology up to 1 mm in length grew overnight. Crystals of the other phases were not obtained in this way but by solvothermal recrystallization. Fifty milligrams of each sample was placed with 0.5 mL of the acetone/water mixture and sealed under vacuum in a thick-walled Pyrex tube. The tubes were heated in an oil bath up to about 100 °C until complete dissolution of the product and then slowly cooled and isothermed as soon as crystal germs started to appear. Crystals up to 3 mm in length were so obtained. Small well-developed crystals with dimensions as isotropic as possible were chosen, and their quality checked by the Laue method prior to data collection with the CCD diffractometer.

Structure Determination. The intensity statistics indicated unambiguously a centrosymmetric structure. The structures were solved in space group *P*-1 by the Patterson method, which gave the position of the adamantane cluster. The remaining nitrogen and carbon atoms were gradually found from sequential difference Fourier syntheses, alternating with least-squares refinement of the incomplete structure. The hydrogen atoms were placed geometrically and refined with a riding model and with the constraint $U_{iso} = 1.2U_{eq}$ of the parent carbon atom. All non-hydrogen atoms were eventually refined anisotropically. A summary of crystallographic data for all four compounds is given Table 1.

Structure Description. The four compounds investigated here present essentially the same structural features. They contain very regular $[Ge_4S_{10}]^{4-}$ anions, illustrated in Figure 6, whose interatomic distances agree well with the values reported in the literature for $Na_4Ge_4S_{10}$ [26] with, on average, a terminal Ge−S distance of 2.12 Å and bridging Ge−S distance of 2.23 Å. These adamantane $[Ge_4S_{10}]^{4-}$ clusters are not linked to each other and form a planar array of approximate hexagonal packing, every cluster being surrounded by six neighbors, as shown in Figure 7. The average distance between the centers of two neighboring clusters is close to 10.4 Å, and the close contacts involve S−S distances ranging from 5.11 to 5.62 Å. Such a hexagonal array of the anionic species is also found, for example, in bisdodecylammonium tetrachlorozincate.[17]

The inorganic planes of $[Ge_4S_{10}]^{4-}$ are separated by a bilayer of interdigitated surfactant chains arranged in an antiparallel way; see Figure 8. The width of the constant layer which comprises the adamantane clusters, the trimethylammonium heads, and the first three carbon atoms of the alkyl chains is 12 Å for every C*n*GS phase. The thickness *D* of the interdigitated organic layer increases linearly with *n* as $D = -3.2 + 1.085n$ (Å). As the length *L* of an extended surfactant chain is given by Tanford's law[30] $L = 1.5 + 1.265n$ (Å), the average inclination angle α of the chains with respect to the inorganic plane is $\alpha = \arcsin(1.085/1.265) = 59°$. The distance between the planes of $[Ge_4S_{10}]^{4-}$ anions can therefore be easily tuned in the mesoscopic length scale simply by choosing a starting surfactant of the appropriate chain length.

Half of the alkyl chains are almost fully extended, with internal rotation angles close to 180° and a nitrogen to terminal carbon distance equal to 1.26*n* (Å), in agreement with Tanford's law. The remaining chains are, on average, 1.4 Å shorter than the extended ones and have a torsion angle of about 70° between the second, third, fourth, and fifth carbon atoms. The alkylammonium chains in $(n\text{-}C_{10}H_{21}NH_3)_2MnCl_4$ present also such a non linear conformation.[16] The two types of chains in C12GS are illustrated in Figure 9. The packing of the alkyl chains within the bilayer is also roughly hexagonal, each chain having six nearest neighbors, see Figure 10. A great number of interchain

(30) Tanford, C. *The Hydrophobic Effect: Formation of Micelles and Biological Membranes*; Wiley: New York, 1980; p 52.

Table 1. Crystallographic Data and Details for Structure Solution and Refinement for $[C_nH_{2n+1}N(CH_3)_3]_4Ge_4S_{10}$ Phases with n = 12, 14, 16, and 18

compound name	C12GS	C14GS	C16GS	C18GS
formula	$C_{60}H_{136}N_4Ge_4S_{10}$	$C_{68}H_{152}N_4Ge_4S_{10}$	$C_{76}H_{168}N_4Ge_4S_{10}$	$C_{84}H_{184}N_4Ge_4S_{10}$
fw (g)	1525	1637	1749	1861
a (Å)	10.2442(6)	10.3039(5)	10.2813(6)	10.2667(6)
b (Å)	18.307(1)	18.5006(9)	18.394(1)	18.418(1)
c (Å)	23.006(1)	25.021(1)	26.690(2)	28.626(2)
α (deg)	72.363(1)	105.533(1)	100.573(1)	83.114(1)
β (deg)	83.666(1)	95.832(1)	95.463(2)	84.951(1)
γ (deg)	89.901(1)	90.175(1)	90.038(1)	89.910(1)
Z, V (Å^3)	2, 4084.5(4)	2, 4569.5(4)	2, 4938.3(5)	2, 5352.9(5)
λ	Mo Kα	Mo Kα	Mo Kα	Mo Kα
space group	P-1	P-1	P-1	P-1
d_{calc}	1.240	1.190	1.176	1.155
μ (mm^{-1})	1.75	1.57	1.45	1.35
crystal dimens (mm^3)	0.40 × 0.30 × 0.15	0.50 × 0.30 × 0.20	0.40 × 0.40 × 0.20	0.60 × 0.30 × 0.15
2θ max (deg)	46.8	46.8	46.6	46.7
temp (°C)	−120	20	20	20
total no. of data	17305	19157	19837	21368
no. of unique data	11306	12555	13139	14223
R_{int} (%)	2.43	2.13	4.91	6.15
data with $F_o > 4\sigma(F_o)$	10173	9716	7644	8402
no. of parameters	703	787	859	931
final $R1$/$wR2$ (%)[a]	3.86/9.53	3.16/7.19	6.26/11.23	6.01/12.20
min/max residue (e$^-$/Å^3)	−0.66/0.91	−0.36/0.44	−0.50/0.58	−0.75/0.81

[a] $R1 = \sum||F_o| - |F_c||/\sum|F_o|$. $wR2 = \{\sum[w(F_o^2 - F_c^2)^2]/\sum[w(F_o^2)^2]\}^{1/2}$.

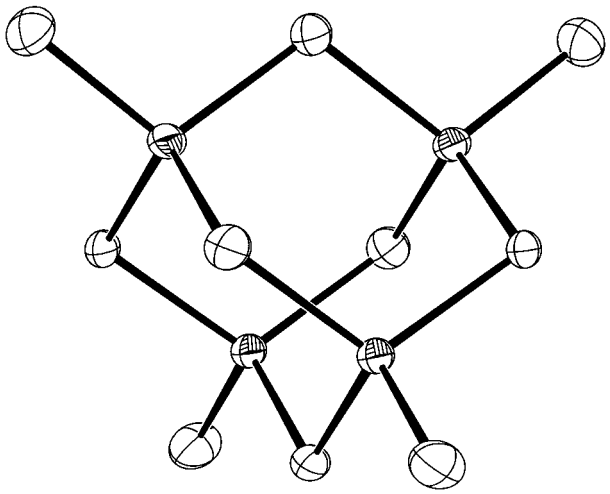

Figure 6. ORTEP representation of the $[Ge_4S_{10}]^{4-}$ cluster in C12GS (drawn with 50% probability ellipsoids).

CH_2/CH_2 van der Waals contacts around 4.2 Å contribute to the stability of the organic layer.

No solvent molecules were found in the crystal structures. The calculation of the Connoly surfaces[31] and the solvent-accessible surfaces[32] of the CnGS phases did not show any void space susceptible to accommodate even a water molecule. This is consistent with the TGA experiments, presented in Figure 11, which do not show any weight loss up to a least 160 °C.

Thermal Properties. TGA and DSC experiments carried out under nitrogen show that the CnGS compounds are relatively thermally unstable and decompose before melting. Whereas the pure surfactants CnBr have a melting or decomposition temperature around 240 °C, the CnGS phases start to decompose at about 180 °C, regardless of the alkyl chain length. This relative instability might be due to the large size of the $[Ge_4S_{10}]^{4-}$ anion which lowers the charge density on the polar interfaces, thus reducing the overall stability of the compound. Above 450 °C, the weight loss is complete and the remaining product is amorphous GeS_2, which is consistent with the percentage of mass lost for every CnGS compound.

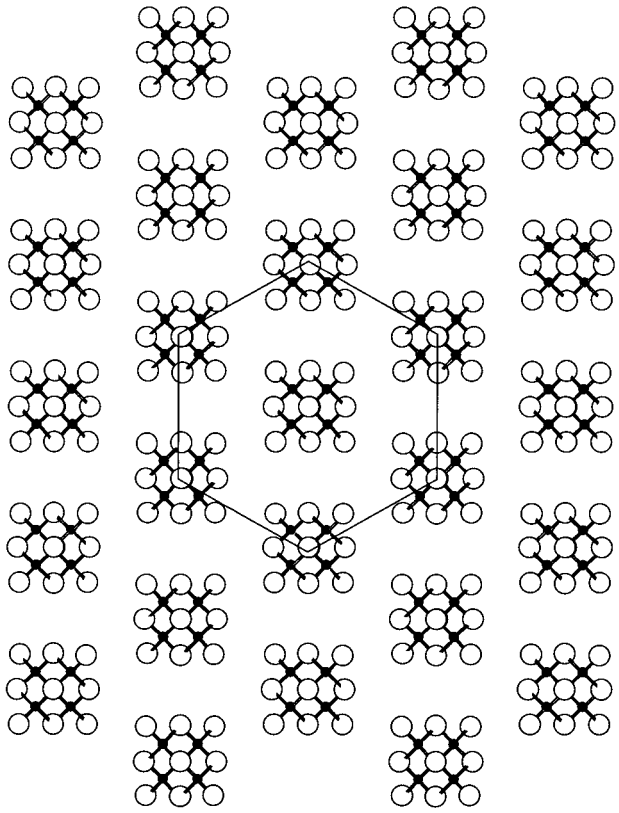

Figure 7. Pseudo-hexagonal two-dimensional packing of the $[Ge_4S_{10}]^{4-}$ clusters in C14GS. The overlaid hexagon is used as a guide to the eye.

DSC experiments and subsequent X-ray powder diffraction analyses show that the CnGS phases undergo a reversible solid-state phase transition that takes place at T_t = 169 °C for C12GS (see Figure 12), 152 °C for

(31) Connolly, M. L. *J. Appl. Cryst.* **1983**, *16*, 548.
(32) Spek, A. L. *Acta Crystallogr.* **1990**, *A46*, C34.

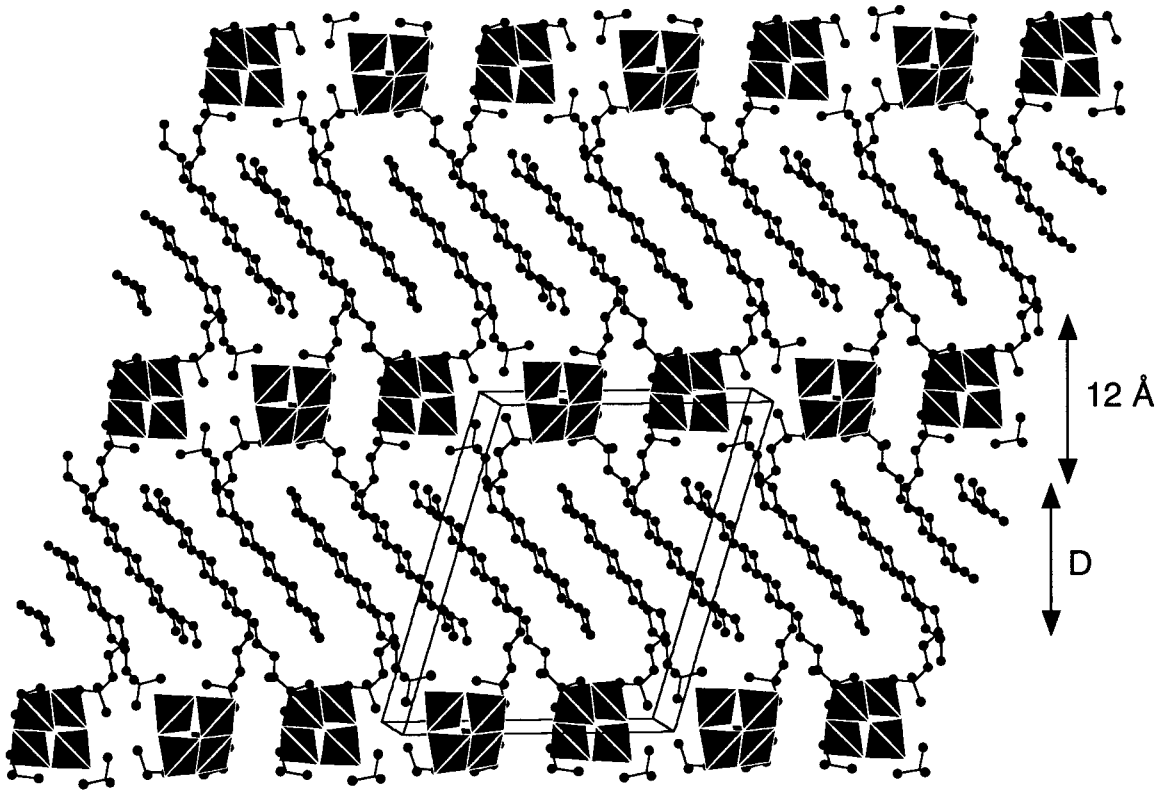

Figure 8. Overall structure of C12GS; H atoms omitted.

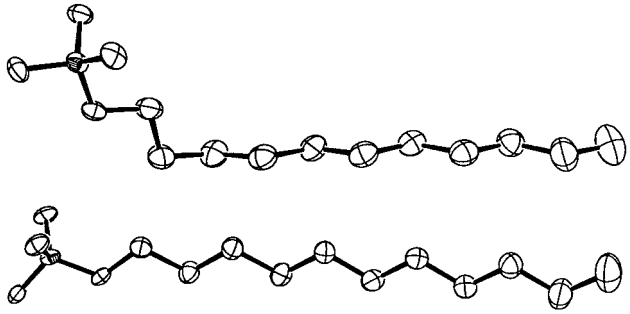

Figure 9. ORTEP representation of linear and twisted surfactant chain in C12GS; H atoms omitted (drawn with 50% probability ellipsoids).

C14GS, 148 °C for C16GS, and 138 °C for C18GS. This transition temperature therefore depends on *n* in the C*n*GS family. The C*n*Br surfactants show such a transition as well, but in a narrower temperature domain, ranging from T_t = 98 °C for C12Br to 106 °C for C18Br. In any case, the thermal behavior of the C*n*GS phases seems different from that observed for various alkylammonium tetrachlorocobaltates,[5,6] which are said to contain isolated $CoCl_4^{2-}$ tetrahedra. These halogenometalates of general formula $(C_nH_{2n+1}NH_3)_2$-$CoCl_4$ with $n = 9-17$ melt congruently around 167 °C, independently of *n*, but exhibit several solid-state phase transitions occurring between T_t = 72 and 107 °C, T_t increasing with *n*. These phase transitions are always ascribed in the literature to a change of conformation of the alkyl chains. In the C*n*GS family, the organic bilayers are almost fully interdigitated and thus should be relatively rigid. A gain in conformational freedom would then require high energy, and this could explain why the transition and decomposition temperature are comparatively close to each other.

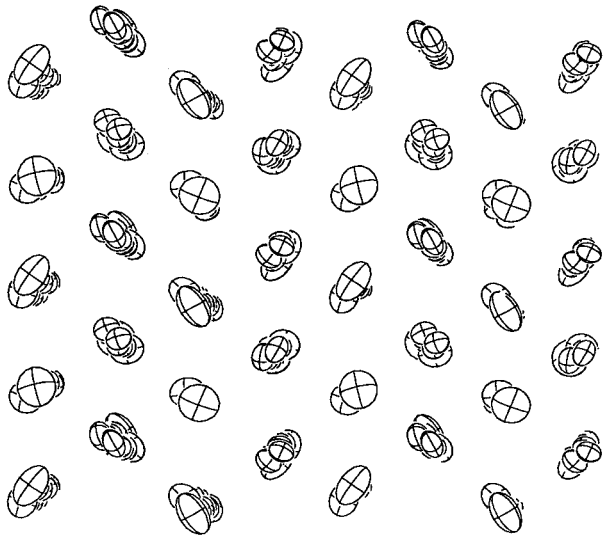

Figure 10. Projection of the alkyl chains within the bilayers, showing their pseudo-hexagonal packing. H atoms omitted.

We did not perform calorimetric experiments below room temperature on these compounds. Nevertheless, the structure of C12GS determined at −120 °C is similar to those determined at room temperature. This indicates that these phases are unlikely to undergo low-temperature structural phase transitions toward a polymorph of lower symmetry.

Reactivity and Absorption Properties. At room temperature the C*n*GS phases exhibit high affinity for linear alcohols of various lengths, from methanol to dodecanol. This absorption (and subsequent desorption) process, which is accompanied by an expansion of the layers, was studied by X-ray powder diffraction by adding drops of alcohol on a thin layer of sample sprayed

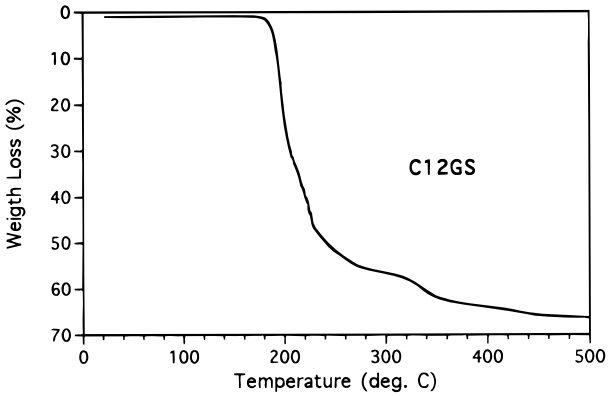

Figure 11. Thermogravimetric analysis of C12GS.

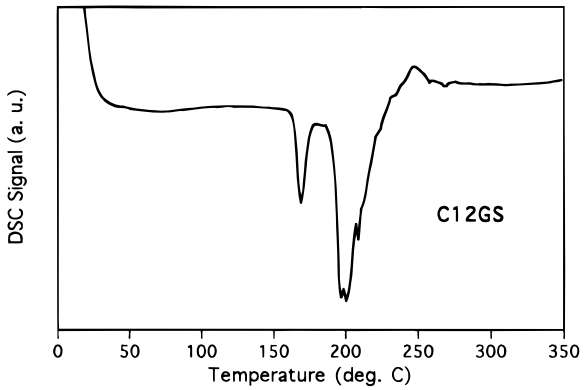

Figure 12. Differential scanning calorimetry analysis of C12GS.

onto a glass slide. The mass absorption, evidenced by the shift of the Bragg peaks, is immediate for methanol and ethanol but becomes sluggish for the long-chain alcohols. Conversely, the desorption takes only few minutes under ambient conditions (in air at room temperature) for the short alcohols but was not observed even for extended periods of time for octanol and beyond. The very high speed of data collection of the INEL CPS120 diffractometer enabled us to observe that, even for methanol, the desorption proceeds in one step, from the "fully charged" back to the original "dry" compound, most likely without an intermediate phase. The reversible absorption of butanol by C14GS is illustrated Figure 13. Because of the high degree of preferred orientation of the powder patterns, we could only observe the increase of the interlayer spacings d_{00l}, reported Figure 14, and not of the other lattice constants. Attempts to study the structure of a C14GS crystal immersed in propanol in a capillary failed because the crystal crumbled upon solvent absorption. Absorption experiments with ethanol/water mixtures with compositions ranging from 1:5 to 5:1 in volume led to the same d_{00l} expansion observed with the pure alcohol. Similar results were obtained with butanol/hexane mixtures. Long alcohol absorbates are quite stable. For example, decanol is absorbed by C14GS, and the product is stable for weeks. It does not desorb after one night under vacuum at room temperature, but it does so within 1 h at about 70 °C in air (oven). Incidentally, we found that these phases do not absorb water, alkanes, or aromatic hydrocarbons, and therefore they could be used in separation applications of alcohols from these solvents.

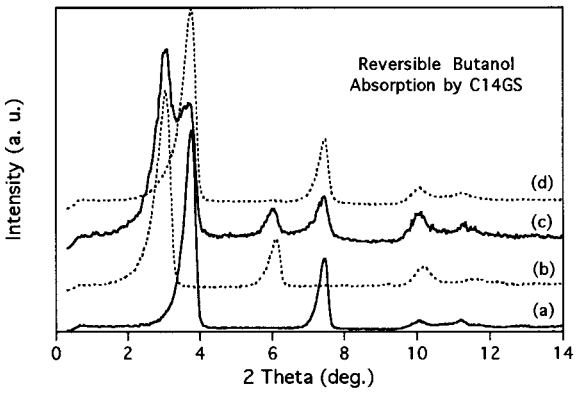

Figure 13. Reversible butanol absorption of C14GS studied by X-ray diffraction: (a) reference pattern, starting compound; (b) 30 s after *n*-butanol absorption; (c) 45 min after *n*-butanol absorption; (d) 90 min after *n*-butanol absorption. At this point complete desorption has occurred with a return to the starting C14GS phase.

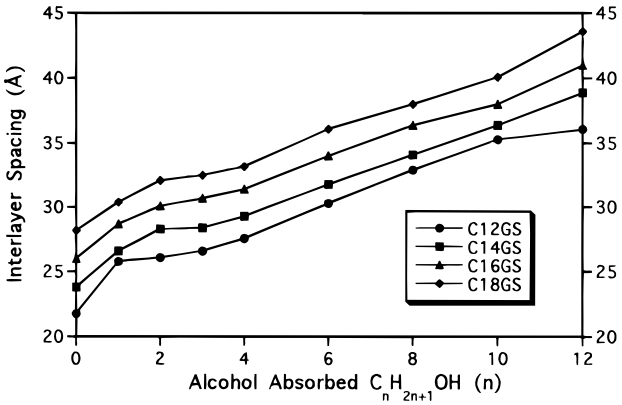

Figure 14. Dependence of the interlayer spacing of C*n*GS upon absorption of alcohols of various lengths.

Concluding Remarks

We have obtained and characterized a new family of surfactant−inorganic phases (C*n*GS) containing planes of well-ordered, unconnected thiogermanate anions. The distance between these inorganic planes is within the mesoscopic range and can be easily tuned. A noteworthy property of these phases is their preferential affinity for various alcohols over water. The C*n*GS phases are potential precursors for the synthesis of mesoporous materials which would contain both surfactant chains and an inorganic framework of cross-linked thiogermanates clusters. Further work aiming at the synthesis of mesoporous compounds is currently under way.[33]

Acknowledgment. Support from the National Science Foundation CHE 96-33798 (Chemistry Research Group) is gratefully acknowledged. Part of this work was carried out using the facilities of the Center for Electron Optics of Michigan State University. F.B. thanks Dr. X. Z. Chen for the EDAX measurements and Mr. J. Hanko for the Raman spectra.

Supporting Information Available: Tables of crystallographic data, fractional atomic coordinates, and anisotropic displacement parameters for compounds $[C_nH_{2n+1}N(CH_3)_3]_4Ge_4S_{10}$ where n = 12, 14, 16, and 18 (33 pages). Ordering information is given on any current masthead page.

CM970755D

(33) Bonhomme, F.; Kanatzidis, M. G. Manuscript in preparation.